Stimulatory current at the edge of an inactive conductor in an electric field: Role of nonlinear interfacial current-voltage relationship

Jared A. Sims[1], **Andrew E. Pollard**[2], **Peter S. White**[3], and **Stephen B. Knisley**[1]

[1] Department of Biomedical Engineering - University of North Carolina at Chapel Hill

[2] Department of Biomedical Engineering – University of Alabama at Birmingham

[3] Department of Chemistry – University of North Carolina at Chapel Hill

Abstract

Cardiac electric field stimulation is critical for the mechanism of defibrillation. The presence of certain inactive epicardial conductors in the field during defibrillation can decrease the defibrillation threshold. We hypothesized this decrease is due to stimulatory effects of current across the interface between the inactive conductor and the heart during field stimulation. To examine this current and its possible stimulatory effects, we imaged transmittance of indium-tin-oxide (ITO) conductors, tested for indium with x-ray diffraction, created a computer model containing realistic ITO interfacial properties, and optically mapped excitation of rabbit heart during electric field stimulation in the presence of an ITO conductor. Reduction of ITO to indium decreased transmittance at the edge facing the anodal shock electrode when trans-interfacial voltage exceeded standard reduction potential. The interfacial current-voltage relationship was nonlinear, producing larger conductances at higher currents. This nonlinearity concentrated the interfacial current near edges in images and in a computer model. The edge current was stimulatory, producing early postshock excitation of rabbit ventricles. Thus, darkening of ITO indicates interfacial current by indium reduction. Interfacial nonlinearity concentrates current near the edge where it can excite the heart. Stimulatory current at edges may account for the reported decrease in defibrillation threshold by inactive conductors.

Keywords

passive conductor; indium-tin-oxide; heart; defibrillation; excitation; computer model

INTRODUCTION

Cardiac electric field stimulation is critical for the mechanism of defibrillation.[1] The role of the intracardiac voltage gradient generated during the shock has been emphasized in experimental studies and in modeling studies of lead positions used in defibrillation.[2] Activating function theory suggests the effects of electric fields are complex, and include specific roles of the spatial variation in the voltage gradient and of the spatial variation in conductance.[3]

We have recently reported that the presence of certain inactive epicardial conductors in the field during defibrillation can decrease the defibrillation threshold.[4] An inactive conductor

Address for correspondence: Stephen B. Knisley, University of North Carolina at Chapel Hill, Department of Biomedical Engineering, 152 MacNider Hall, CB #7575, Chapel Hill, North Carolina 27599, sknisley@email.unc.edu, Phone: 919-966-6653.

(i.e., an electrically conductive object or wire that is not attached to a current generator) on the heart can produce cardiac stimulatory current during a DC defibrillation-type electric field.[5–7] Stimulation was shown to occur by current in an inactive wire contacting the heart.[6] Such effects may be important for electrodes or conductive devices implanted in the body, and for new devices that may enhance effectiveness of biological applications of electric current. However, little is known about the factors that determine the magnitude and spatial distribution of stimulatory current produced by inactive conductors.

We hypothesized that the voltage gradient is the driving force for current that enters or exits each point on the surface of an inactive conductor. Then the width of the inactive conductor in the direction of the electric field would be a determinant of the current because the potential difference between edges of a conductor will increase for a conductor that spans a greater distance in the direction of the field. Since conductance of the interface of a conductor with the tissue may vary with current strength,[8–11] we also hypothesized that variations in the conductance influence the distribution of current on an inactive conductor. Previous analyses of current distribution on a unipolar electrode or inactive conductor did not incorporate variations in the interfacial conductance.[5, 10, 12]

Our previous studies of current distribution on conductors in an electric field or unipolar electrodes utilized the product of transmittances of excitation and fluorescence light through an indium-tin-oxide (ITO) film to evaluate current distribution.[5, 10] ITO films have high transmittance and electrical conductivity, and can be lithographically patterned. These properties have enabled simultaneous optical and electrical mapping of cardiac excitation and responses to electrical stimulation.[5, 10, 13–15] The extent to which measurement of the distribution of stimulatory current is practical using transmittance of ITO film has broad implications for improved understanding of the interactions between shocks and tissue. Therefore one goal of this study was to explore the method of current measurement. We approached this by using a more direct measure of transmittance than was used previously, [5, 10] and by determining the electrochemical process by which the transmittance decreases with current. Another goal was to test the hypothesis that width of the inactive conductor in the direction of the electric field and variations of interfacial conductance as a function of current strength influence the distribution of current at the edges. Since there was no prior data for ITO indicating the interfacial conductance as a function of current strength, we measured this. The final goal was to examine optical maps of the effect of an inactive conductor on excitation by field stimulation of the rabbit ventricle stained with transmembrane voltage-sensitive fluorescent dye.

METHODS

Production of conductors

ITO was sputtered onto one side of a 5 cm × 7.5 cm borosilicate glass plate (Thin Film Devices, Anaheim, CA). Thickness of the plate was 1.1 mm and thickness of ITO film was 850 nm. Nonuniformity of the film was ±5%. The sheet resistance was 1–2 ohms per unit square region of the plate (a standard unit for sheet resistance).[16] Plates were then cut to a desired size or photolithographically patterned for different experiments.

X-ray powder diffraction

To examine the electrochemical change that decreases transmittance of ITO, x-ray powder diffraction was performed on plates before and after application of current. A copper wire was attached with conductive cement to one edge of a 2.5 cm × 3.75 cm ITO plate. A 4.7 cm^2 area of the plate opposite the wire was immersed in 3 liters of Tyrode's solution containing (in mM) 129 NaCl, 4.5 KCl, 1.8 $CaCl_2$, 1.1 $MgCl_2$, 26 $NaHCO_3$, 1 Na_2HPO_4, 11

glucose, 0.04 g/L bovine serum albumin. This solution was identical to the solution used in our previous studies of ITO.[5, 10] The solution was stirred vigorously and kept at 22 degrees.

The ITO was the cathode while a 5 cm silver wire in the solution was the anode (Figure 1A). A pulse train generator (Pulsemaster A300, World Precision Instruments, Sarasota, FL) and custom current source were used to apply current pulses of 234 mA with duration 10 msec. A train consisting of 89 pulses at a rate of 1 pulse per second was applied. In the results shown, the plate received 6 trains for a total of 534 cathodal pulses.

X-ray powder diffraction was performed with a Rigaku Multiflex (Rigaku Corporation, Tokyo, Japan) using Ni-filtered Cu radiation generated at 40 kV and 40 mA. Scans were performed at degree change in 2 theta per minute. The x-ray beam irradiated an area of approximately 1 cm^2. The diffraction patterns with and without application of the pulses (Figure 1 B and C) were compared with computed patterns.[17]

Measurement of transmittance

ITO thin films were patterned using photolithographic methods to produce conductive strips having widths of 0.1, 0.5, 1 and 5 mm.[5] A 1 cm^3 cubical polystyrene cuvette was filled with 0.9% sodium chloride solution. This solution was chosen because its conductance is well-known.[18] Two stainless steel mesh electrodes were placed at opposite sides of the cuvette to deliver an electric shock. One of the ITO conductors was positioned on the top surface of the solution and oriented with its edges parallel to the top and bottom edges of the shock electrodes (Figure 2A). An incandescent lamp illuminated the cuvette while a microscope with a numerical aperture 0.23 and a digital camera above the cuvette acquired transillumination images of the conductor (Nikon SMZ-10A, Tokyo, Japan). Shocks having duration of 10 msec were given from the mesh electrodes at an initial current strength of 500 mA. If no change in transmittance was seen, strength was increased to 880 mA. Photos were taken before and after shocks, and then converted to grey scale. Images with ITO were normalized by dividing by an image with glass having no ITO. This method indicated transmittance without requiring computation of the square root of the intensity.[5, 6]

Measurement of interfacial conductivity

The conductance of the interface of ITO and 0.9% sodium chloride (2 experiments) or Tyrode's solution (1 experiment) was measured with a three-lead method (Figure 6A). A wire lead was attached with conductive cement to a 5 cm × 7.5 cm glass plate containing ITO film. This lead was used to pass current to the ITO. A plastic cylinder with a height of 20 mm and inside diameter of 9.4 mm was attached to the ITO with nonconductive epoxy and filled with the solution. A coil wire was placed near the top of the solution. With this arrangement, current flowed between a circular area of ITO at the bottom of the cylinder and the coil at the top. A third lead was used to measure the potential in the solution near the ITO. For this, an insulated silver wire with a diameter of 0.011 mm was lowered into the solution using a micromanipulator. The distance from the cut end of the wire to the ITO surface was 1 mm in the experiments that used 0.9% sodium chloride solution and 50 micrometers in the experiment that used Tyrode's solution.

Current of either polarity was injected across the interface of ITO and solution using the ITO lead and the coil. The voltage between the ITO and the silver wire was measured with a unity gain precision isolation amplifier (Analog Devices, Model AD210) with bandwidth DC to 16 KHz using a digital oscilloscope that was calibrated in 2008 at the factory (Tektronix, Model TDS3032B). This measurement overestimates the interfacial voltage by an error voltage, which is the voltage between the silver wire and the solution adjacent to the

ITO. To correct this in the experiments with 1 mm between the wire and the ITO, we subtracted error voltages that were calculated from the 0.9% sodium chloride resistivity of 71 ohm cm, area of ITO contacting sodium chloride and distance between the silver wire and the ITO.[18] In the experiment with a distance of 50 micrometers, the error voltage was less than 1% of the measured voltage and was not subtracted. The conductivity of the interface of ITO with the solution was then calculated using the interfacial voltage, current strength and area of the interface of ITO and solution.

Computer model of inactive conductor in electric field

To provide insights into the electrical and optical observations associated with field stimulation of the different ITO constructs, we used simplified computer models whose components accounted for the major structural components of the experimental arrangement (Figure 5A). To represent the conducting solution, we used 1000 resistive elements placed end-to-end. Each solution element measured $10\times10\times10000$ μm^3, with the largest dimension representing conducting solution thickness. We prescribed a resistance of 50 ohms for each conducting solution element to take into account an approximate solution resistivity (50 ohm cm) and the 10×10000 μm^2 surfaces through which supplied current flowed during field stimulation. To represent the ITO layer, we used 500 resistive elements placed end-to-end parallel to the central conducting solution elements. Each ITO element measured $10\times10\times0.85$ μm^3. We prescribed a resistance of 2 ohms for each ITO element to take into account the sheet resistance for the material at this thickness and the 10×0.85 μm^2 surfaces separating adjacent elements.

We then considered three different possibilities for the interface between the conducting solution and ITO elements. This interface was assumed noncapacitive, as the approach to stimulation in the experiments involved use of a DC pulse of sufficiently long duration to limit any capacitive contribution at the electrode-electrolyte interface in the response. In experimental measurements, we found the capacitive time constant of the ITO to be ~0.25 msec, which was considerably shorter than our shock duration of 10 msec.

First, we prescribed a constant interfacial resistance of 11.36 Mohm between conducting solution and ITO elements. This resistance was derived from the interfacial conductivity during anodal stimulation of an ITO disk in saline as reported by Liao et al.,[10] scaled to account for a reduction in surface area to 10×10 μm^2. Second, we prescribed two constant interfacial resistances on opposite sides of the model's midpoint to reflect the differences in interfacial conductivity between anodal and cathodal stimulation reported by Liao et al.[10] Taking these differences into account, we used an interfacial resistance of 11.36 Mohm in the part of the model located closest to the cathodal shock electrode, which established the inactive conductor as an anode, and an interfacial resistance of 6.67 Mohm in the part of the model located closest to the anodal shock electrode, which established the inactive conductor as a cathode.

The final possibility we considered took into account our observation that the interfacial conductivity decreased with a reduction in supplied current during both anodal and cathodal stimulation. This decrease and the reported difference in the conductivity for different polarities were approximated by the following linear relationships:

$$R_c = \frac{1}{15.6\times10^{-9}+0.3i} \quad (1)$$

$$R_A = \frac{1}{8.8 \times 10^{-9} - 0.3i} \quad (2)$$

where R_C is the cathodal resistance, R_A the anodal resistance and i is the current.

For our simulations, we initially prescribed 11.36 Mohm in the part of the model located closest to the cathodal shock electrode and 6.67 Mohm in the part of the model located closest to the anodal shock electrode. Current supplied between the two shock electrodes gave rise to potential differences across the interface between each conducting solution and ITO element, as expected. Each potential difference was then used to calculate a component current, which was then used with Equation 1 or 2 to adjust the interfacial resistance based on the magnitude of the component current. Shock application then gave rise to a new set of potential differences. This process was repeated until the potential differences changed by less than 0.001 mV from the potential differences recorded during the previous iteration.

Bipolar electrode measurements

The distribution of the vertical component of the current density in the solution above the ITO was estimated using bipolar potential measurements. A 1 cm^3 polystyrene cuvette with shock electrodes on opposite sides was cemented to a glass plate containing a 5 mm wide ITO strip (Figure 7A). The cuvette was filled with 0.9% sodium chloride solution. Two enamel-coated tungsten wires with diameter 50 micrometers were cemented parallel to one another with the tips 0.5 mm apart to create a bipolar measurement electrode. The electrode was oriented vertically and lowered into the cuvette to within ~0.25 mm from the glass. The electrode was initially near the cathodal shock electrode above an area of glass not covered with ITO, and was then moved in 0.625 mm increments toward the anodal shock electrode. At each position, a shock of 500 mA and 10 msec was given through the shock electrodes and the bipolar voltage difference was measured with the unity gain amplifier and digital oscilloscope.

Experiment with rabbit heart

Experiments were performed with anterior and posterior ventricular epicardium of a rabbit heart to determine whether the edge of an inactive conductor excites tissue during electric field stimulation. The heart was isolated from a New Zealand White Rabbit according to a protocol approved by the Institutional Care and Use Committee of The University of North Carolina at Chapel Hill and perfused with Tyrode's solution containing the transmembrane voltage-sensitive fluorescent dye, di-4-ANEPPS.[5] Stainless steel mesh shock electrodes were positioned epicardially 2 cm apart and on either side of the conductor to apply field stimulation. An ITO disc having a diameter of 1 cm was produced lithographically on a glass substrate. The glass was held on the epicardium with a micromanipulator and was moved laterally in different trials so that either the conductor or part of glass that did not contain the conductor contacted epicardium between shock electrodes. A laser scanner system was used to perform dual- wavelength ratiometric optical mapping at 128 spots in a 6 mm × 12 mm grid encompassing edges of the conductor facing the shock electrodes. Field stimulation was applied in electrical diastole with a cycle length of 300 msec, pulse duration of 5 msec, alternating polarity and strength of 30–1,000 mA in 11 steps.

RESULTS

X-ray powder diffraction

X-ray powder diffraction patterns were measured for ITO films that were treated with cathodal current across the Tyrode's solution interface or no current (control). The measured

diffraction patterns were fitted to computed diffraction patterns for indium and indium oxide. The fitting reports consisted of 12–14 peaks and gave residual error of fit from 2.5 to 4.3 %. Indium was indicated by peaks in the pattern for the treated ITO that were also present in the computed pattern for indium, but were absent in the control pattern. The major peaks meeting this criterion in the film treated with 534 pulses were located at 32.9 and 35.7 degrees (asterisks in Figure 1C). No signs of strong peaks of the computed patterns for tin or tin oxide were found in the measured patterns.

Transmittance

Figure 3A shows the cropped digital photos of the 5 mm ITO conductor before shocks, after 1 shock and after 3 shocks. The shock strength was 500 mA. The first shock darkened the edge of the conductor nearer the anodal shock electrode. Repetitions of the shock further darkened the edge. These shocks also produced bubbles at the edge nearer the cathodal shock electrode that increased with repetitions of the shock.

Figure 3B shows the transmittance for one horizontal row of pixels near the center of each image. The greatest change in transmittance occurred at the edge of the ITO nearer the anodal shock electrode. The decrease in transmittance seen after three shocks was localized to a 1.2 mm region near the edge of the ITO. Variations in the intensity near the edge facing the cathodal shock electrode were produced by bubbles that scattered light.

Figure 4A shows the cropped digital photos for the 1 mm ITO conductor before shocks, after three shocks of 500 mA and after an additional shock of 880 mA. No change in transmittance was observed after any of the 500 mA shocks. After the shock of 880 mA, a change in transmittance was seen at the edge nearer the anodal shock electrode. This decrease was localized to a sub-millimeter region. Magnification of the image after the 880 mA shock indicated bubbles at the edge of the ITO nearer the cathodal shock electrode.

The images for the 0.1 and 0.5 mm wide ITO conductor did not show a change in transmittance for either a 500 or 880 mA shock. Also 20 repetitions of the 880 mA shock did not affect transmittance of the 0.1 or 0.5 mm conductors.

Computer models with constant interfacial conductances

In the model with a single value for the interfacial conductivity across the 5 mm conductor, the current varied linearly with distance across the entire conductor. In the model with different values for each half, the interfacial current varied linearly with a change in the slope at the midpoint of the conductor where conductivity changed. Since the models with constant values of interfacial conductivity did not predict the abrupt rise of current at edges found experimentally (Figures 3 and 4), we performed measurements of the interfacial current-voltage relationship to see if constant values were appropriate.

Interfacial conductance

The slopes of the plots of current vs. potential increased with increases in the current strength (Figure 6). When the ITO was the anode (left side of the graph), the rise in slope began when the magnitude of voltage exceeded a threshold of 2.5 V (average from the 2 experiments that included small currents shown as open boxes and plus signs in Figures 6B and 6C). When the ITO was the cathode (right side), the rise in slope began when the magnitude of the voltage exceeded an average threshold of 1.5 V.

Figure 5B shows the interfacial conductivity of ITO versus current density measured in two experiments (symbols). For both polarities of current, the conductivity increased with

increases in current strength. This increase was more pronounced for the cathodal current (right side of Figure 5B).

Computer model with nonlinear interfacial current-voltage relationship

An additional model incorporated the variable conductivity (Equations 1 and 2). Figure 5C shows that interfacial current density was not linear over the entire width, but was localized near the edges. To confirm that conductivities in the converged iteration of the model were similar to measured values, effective conductivities at interfacial elements in the model were also plotted (dots in Figure 5B). (These values were calculated as the interfacial current at each element of the modeled conductor divided by the voltage difference between the conductor and the adjacent solution, and finally divided by the area of the element.)

Current distribution estimated with bipolar electrode

Figure 7B shows the potential difference measured with the roving bipolar electrode during shocks. This difference is proportional to the vertical component of current density. The component is largest near edges of the ITO. The center of the graph had a reduced slope similar to the model that incorporated a nonlinear current-voltage relationship.

Stimulation of rabbit heart

Stimulation by the edge of an ITO conductor in an electric field was tested in two regions of rabbit epicardium for both shock polarities. The stimulation threshold for excitation of the tissue at the cathodal shock electrode was 2.3±1.4 mA (n=4, not shown). For shocks just above that threshold, early excitation occurred near the cathodal shock electrode. The edge of the ITO did not produce early excitation for such weak stimulation. When the shock strength was increased, latency of excitation (time from onset of shock to steepest part of phase zero depolarization) in the tissue near the ITO conductor decreased, reaching 0–1 msec for a 1 A shock. In all four cases, there was an intermediate range of shock strengths centered at 62±26 mA in which tissue near the edge of the ITO facing the anodal shock electrode had smaller latency when the ITO was on the heart vs. without the ITO. An example is illustrated in the right part of maps in Figure 8 where the latency was 3 msec with the ITO and 8 msec without it. For all cases, the greatest difference in this latency with and without the ITO was 5.1±2.5 msec (p=0.027, n=4). The edge of the ITO facing the cathodal shock electrode did not noticeably affect latency (left part of the maps).

DISCUSSION

Electrochemical reactions

The x-ray powder diffraction indicates cathodal current reduces indium on the film. When current flows from solution to ITO, indium oxide is reduced to indium according to the following reaction.[19]

$$In_2O_3 + 3H_2O + 6e^- \Rightarrow 2In + 6OH^-$$
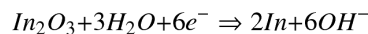
The decrease in transmittance resulting from indium formation occurs at the edge of the conductor facing the anodal shock electrode (right edge in Figure 3A).

When current flows from ITO to solution, oxidation can form oxygen gas by electrolysis of water.[20]

$$2H_2O \Rightarrow O_2 + 4H^+ + 4e^-$$
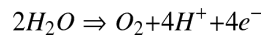
The resulting bubble formation and scattering of light at the left edge of the conductor (visible in the right image of Figure 3A) is consistent with the electrolysis.

Thresholds for interfacial current

The standard reduction potential for indium is −1.034 V, whereas the standard potential for water electrolysis is 1.23 V. These potentials differ from the threshold interfacial voltages that had to be exceeded in order for substantial currents to occur (1.5 V and 2.5 V for the respective currents in Figures 6B and 6C). The standard potentials may be smaller because they apply to equilibrium conditions.

The voltage gradient times half of the conductor width predicts the magnitude of interfacial voltages at the edges. Whether there is observable interfacial current will depend on this value exceeding the thresholds. For example, the calculated voltage gradient in Figure 3 (35.5 V/cm) times 0.25 cm yields 9 V. This prediction exceeds the thresholds for current. Indium and bubbles confirm presence of current. However the voltage gradient times half of the conductor width for the 500 mA shock in Figure 4 is only 1.78 V. This is smaller than the example above because the conductor width is only 1 mm. The prediction that interfacial voltages are subthreshold for current is confirmed by absence of indium or bubbles. With a shock of 880 mA in Figure 4 the predicted interfacial voltage is 3.1 V. The superthreshold prediction again determines presence of current, as confirmed by indium and bubbles.

The magnitude of the threshold is greater when the ITO is the anode (left side of Figures 6B and 6C). It is possible this asymmetry occurs because of the greater oxidation potential compared with the reduction potential. Also the slope increases at greater potentials, effectively increasing interfacial conductivity. This increase is consistent with an exponential rise in current at higher voltages as described by the Butler-Volmer equation. [21]

Impact of interfacial conductance on current distribution of inactive conductor

Since the field potential varies across the conductor, interfacial current density would be nonuniform and would have maxima at edges even if interfacial conductivity is constant. However, since interfacial conductivity increases with current density, the conductivity may be greatest at edges (Figures 5B, 6B and 6C). Our model having conductivity that varies as a function of current indicates that the increase in conductivity at edges further concentrates current there (Figure 5C). The validity of that model is supported by the images for the 5 mm conductor, in which current is localized within approximately the first millimeter from the right edge (Figure 3), as it is in the model. This model is further supported by Figure 7B showing the vertical potential gradient above ITO is largest near edges of the ITO.

We are not aware of another realistic model that reproduces the edge effects in our images. Preliminary models with constant interfacial resistance ranging over 6 orders of magnitude, (not shown) indicated that a model having very low resistance, 11.36 Kohms, for each interfacial element would produce edge current distributions comparable to those in images. However that model is not realistic because the measured range of interfacial resistance is several orders of magnitude higher than the value used in the model (Ref. 10 and present measurements).

Implications for interactions between shocks and tissue

The results in the right part of maps in Figure 8 indicate the edge facing the anodal shock electrode can produce excitation in the heart. This is consistent with cathodal current (i.e., reduction) at the right edge of the conductor in Figure 3A. The lack of excitation by anodal current (oxidation) at the left edge may occur because the anodal threshold for excitation of the heart is much higher than the cathodal threshold.[22]

To the best of our knowledge, the model is the first one that incorporates current-dependent conductivity of an electrode interface. Changes in impedance by cardioversion or defibrillation shocks are correlated with respiration, blood volume or edema, contact pressure, interfacial coupling agent, and shock energy.[11, 23, 24] It may be important to incorporate conductivity changes into future models.

An inactive wire conductor can produce stimulation during shocks.[6] Also interfacial current for a 1-cm inactive film conductor alters transmembrane potentials of heart tissue under the conductor.[5] Other studies indicate inactive conductors may affect defibrillation. Large inactive patches either increase the defibrillation threshold, consistent with lowering of the voltage gradient in underlying tissue, or have no effect on defibrillation.[25–28] Our recent work shows inactive silver strips, with a certain amount of edge in the direction perpendicular to the line between shock electrodes, lower the defibrillation threshold.[4] Stimulation by current at the edge may have contributed to that reduction in threshold.

Limitations

A full explanation of the relationship between transmittance and interfacial current may need to take into account the amounts of indium reduced and indium-oxide remaining, and their absorption coefficients. The distribution of current in experiments may vary with distance from the plate, whereas the measurements with the bipolar electrode were limited to a single height above the plate, and the model used a single layer of solution nodes.

The transmittance tests used a conductor having a straight edge, whereas tests in the rabbit heart used a conductor having a curved edge. The role of curvature of a conductor is unknown. However, stimulation occurred where the tangent to the edge faced a shock electrode (3 msec region in Figure 8A). This is the same orientation of edges used in our measurements of transmittance.

Acknowledgments

References

1. Walcott GP, Knisley SB, Zhou X, Newton JC, Ideker RE. On the mechanism of ventricular defibrillation. Pacing Clin Electrophysiol. Feb.1997 20:422–31. [PubMed: 9058846]

2. Aguel F, Eason JC, Trayanova NA, Siekas G, Fishler MG. Impact of transvenous lead position on active-can ICD defibrillation: a computer simulation study. Pacing Clin Electrophysiol. Jan.1999 22:158–64. [PubMed: 9990622]

3. Sobie EA, Susil RC, Tung L. A generalized activating function for predicting virtual electrodes in cardiac tissue. Biophys J. Sep.1997 73:1410–23. [PubMed: 9284308]

4. Sims JA, Knisley SB. Epicardial conductors can lower the defibrillation threshold in rabbit hearts. IEEE Trans Biomed Eng. Apr.2009 56:1196–9. [PubMed: 19272936]

5. Knisley SB, Pollard AE. Use of translucent indium tin oxide to measure stimulatory effects of a passive conductor during field stimulation of rabbit hearts. Am J Physiol Heart Circ Physiol. Sep. 2005 289:H1137–46. [PubMed: 15894581]

6. Girouard S, Ideker R. Passive current redistribution in the heart. J Cardiovasc Electrophysiol. Mar. 2001 12:349–55. [PubMed: 11291810]

7. Patel SG, Roth BJ. How epicardial electrodes influence the transmembrane potential during a strong shock. Ann Biomed Eng. Nov.2001 29:1028–31. [PubMed: 11791674]

8. Ragheb T, Riegle S, Geddes LA, Amin V. The impedance of a spherical monopolar electrode. Ann Biomed Eng. 1992; 20:617–27. [PubMed: 1449230]

9. Das DP, Webster JG. Defibrillation recovery curves for different electrode materials. IEEE Trans Biomed Eng. Apr.1980 27:230–3. [PubMed: 7380438]

10. Liau J, Dumas J, Janks D, Roth BJ, Knisley SB. Cardiac optical mapping under a translucent stimulation electrode. Ann Biomed Eng. Sep.2004 32:1202–10. [PubMed: 15493508]

11. Olsovsky MR, Shorofsky SR, Gold MR. The effect of shock configuration and delivered energy on defibrillation impedance. Pacing Clin Electrophysiol. Jan.1999 22:165–8. [PubMed: 9990623]

12. Wiley JD, Webster JG. Analysis and control of the current distribution under circular dispersive electrodes. IEEE Trans Biomed Eng. May.1982 29:381–5. [PubMed: 7084970]

13. Knisley SB. Evidence for roles of the activating function in electric stimulation. IEEE Trans Biomed Eng. Aug.2000 47:1114–9. [PubMed: 10943061]

14. Knisley SB, Neuman MR. Simultaneous electrical and optical mapping in rabbit hearts. Ann Biomed Eng. Jan.2003 31:32–41. [PubMed: 12572654]

15. Himel HD, Knisley SB. Comparison of optical and electrical mapping of fibrillation. Physiol Meas. Jun.2007 28:707–19. [PubMed: 17664624]

16. Blech, IA. Properties of materials. In: Christiansen, D., editor. Electronics Engineers' Handbook. 4. New York: McGraw-Hill; 1997. p. 9.4

17. White PS, Rodgers JR, Le Page Y. CRYSTMET: a database of the structures and powder patterns of metals and intermetallics. Acta Crystallogr B. Jun.2002 58:343–8. [PubMed: 12037354]

18. Vanysek, P. Equivalent conductivity of electrolytes in aqueous solution. In: Lide, DR., editor. CRC handbook of chemistry and physics. 80. Boca Raton: CRC Press LLC; 1999. p. 5-93.

19. Vanysek, P. Electrochemical series. In: Lide, DR., editor. CRC handbook of chemistry and physics. 80. Boca Raton: CRC Press LLC; 1999. p. 8-21-8-26.

20. Kotz, JC.; Paul Treichel, J. Chemistry and Chemical Reactivity. 4. Fort Worth: Saunders College Publishing; 1999.

21. Bockris, JOM.; Reddy, AKN.; Gamboa-Aldeco, M. Modern electrochemistry. Second edition. Fundamentals of electrodics. Vol. 2A. New York: Klewer Academic/Plenum Publishers; 2002. Chapter 7. Electrodics; p. 1066-1068.

22. Lindemans FW, Denier Van der Gon JJ. Current thresholds and liminal size in excitation of heart muscle. Cardiovasc Res. Aug.1978 12:477–85. [PubMed: 719660]

23. Sirna SJ, Ferguson DW, Charbonnier F, Kerber RE. Factors affecting transthoracic impedance during electrical cardioversion. Am J Cardiol. Nov 15.1988 62:1048–52. [PubMed: 3189167]

24. Sirna SJ, Kieso RA, Fox-Eastham KJ, Seabold J, Charbonnier F, Kerber RE. Mechanisms responsible for decline in transthoracic impedance after DC shocks. Am J Physiol. Oct.1989 257:H1180–3. [PubMed: 2801977]

25. Callihan RL, Idriss SF, Dahl RW, Wolf PD, Smith WM, Ideker RE. Comparison of defibrillation probability of success curves for an endocardial lead configuration with and without an inactive epicardial patch. J Am Coll Cardiol. May.1995 25:1373–9. [PubMed: 7722136]

26. Fotuhi PC, Ideker RE, Idriss SF, Callihan RL, Walker RG, Alt EU. Influence of epicardial patches on defibrillation threshold with nonthoracotomy lead configurations. Circulation. Nov 15.1995 92:3082–8. [PubMed: 7586279]

27. Lerman BB, Deale OC. Effect of epicardial patch electrodes on transthoracic defibrillation. Circulation. Apr.1990 81:1409–14. [PubMed: 2317917]

28. Walls JT, Schuder JC, Curtis JJ, Stephenson HE Jr, McDaniel WC, Flaker GC. Adverse effects of permanent cardiac internal defibrillator patches on external defibrillation. Am J Cardiol. Nov 15.1989 64:1144–7. [PubMed: 2816766]
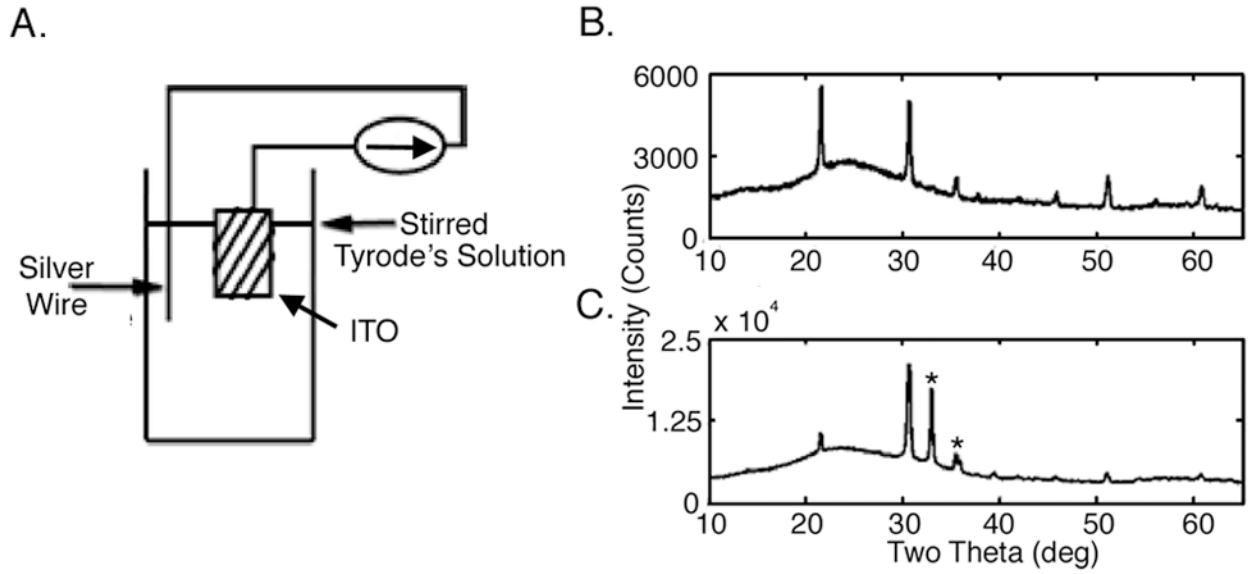
Figure 1.
Experimental setup and x-ray diffraction patterns for indium-tin-oxide (ITO) thin films.
Panel A: Diagram of the preparation of ITO plate to be examined with x-ray diffraction.
Panel B: Pattern from a film that did not receive interfacial current. Peaks found at 21.5, 30.6, 35.5, 37.7, 45.7, 51.1, and 60.7 degrees agree with computed pattern for indium-oxide.
Panel C: Pattern from a film treated with interfacial cathodal current (534 pulses having duration 10 msec and strength 234 mA). The relative magnitudes of several of the indium-oxide peaks decreased (21.5, 45.7 51.1 and 60.7 degrees). New peaks at 32.9 and 35.7 degrees (asterisks) agree with computed pattern for indium.
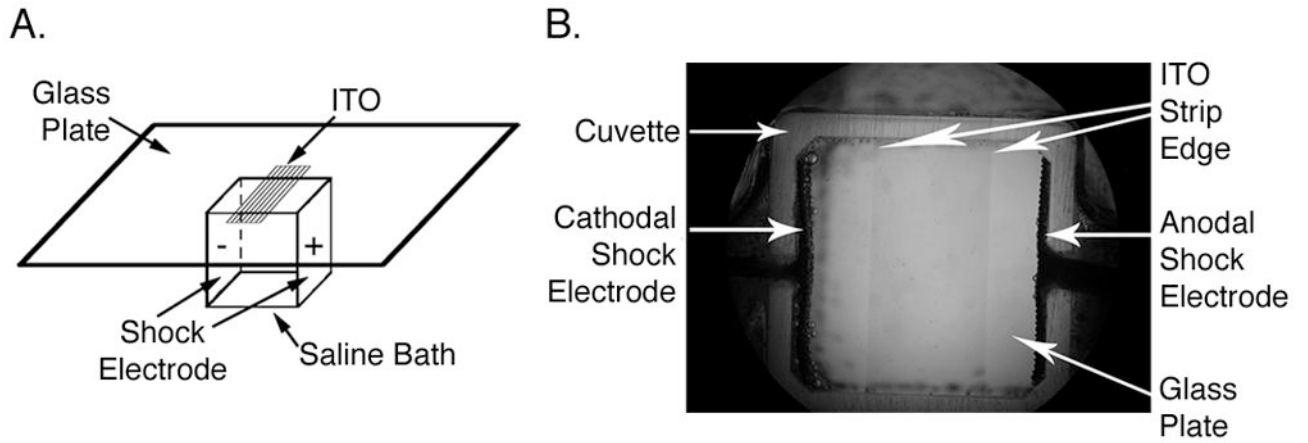
Figure 2.
Experimental setup for indium-tin-oxide (ITO) transmittance measurements. Panel A: Diagram of ITO transmittance setup. A glass plate with rectangular ITO film was placed on top of a saline filled chamber. Shock electrodes were placed on opposite sides of the chamber. Panel B: Image showing full field of view from top. The glass plate covered the entire cuvette containing 0.9 % sodium chloride solution. The edges of the ITO conductor are indicated with arrows. The anodal shock electrode is on the right side of the image and the cathodal shock electrode is on the left side.
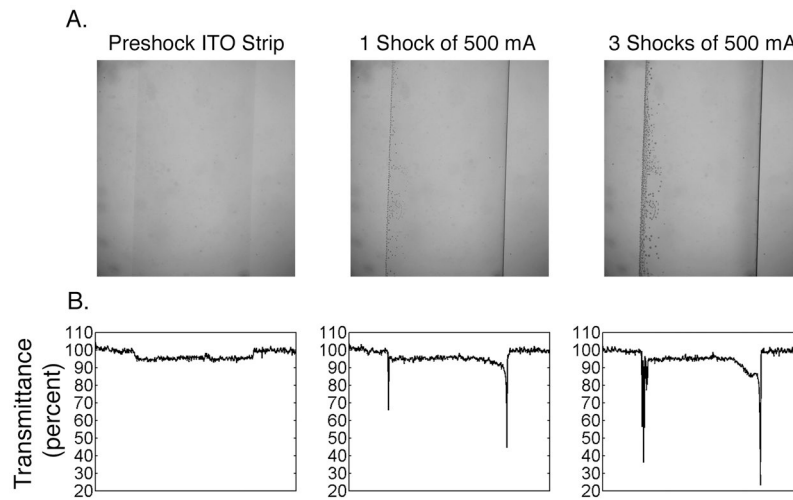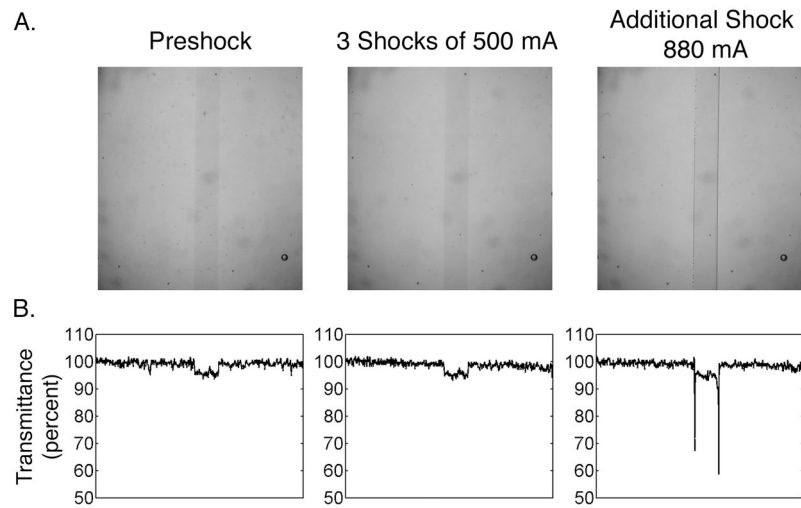
Figure 3.
Transillumination images and transmittance for an inactive indium-tin-oxide (ITO) conductor having a width of 5 mm in an electric field. Panel A: Cropped images obtained before and after shocks. The central image was taken after a single shock of 500 mA. The right image was taken after a total of 3 shocks of 500 mA. Panel B: Transmittance determined as grayscale intensity of horizontal line from images in B after division by the intensity of an image with glass having no ITO on the cuvette.

A.

Preshock   3 Shocks of 500 mA   Additional Shock 880 mA

B.

Figure 4.
Transillumination images and transmittance for inactive indium-tin-oxide conductor having a width of 1 mm in an electric field. Panel A: Cropped images obtained before and after shocks. The central image was taken after three shocks of 500 mA. The right image was taken after an additional shock that had strength of 880 mA. Panel B: Transmittance determined as in previous figure.
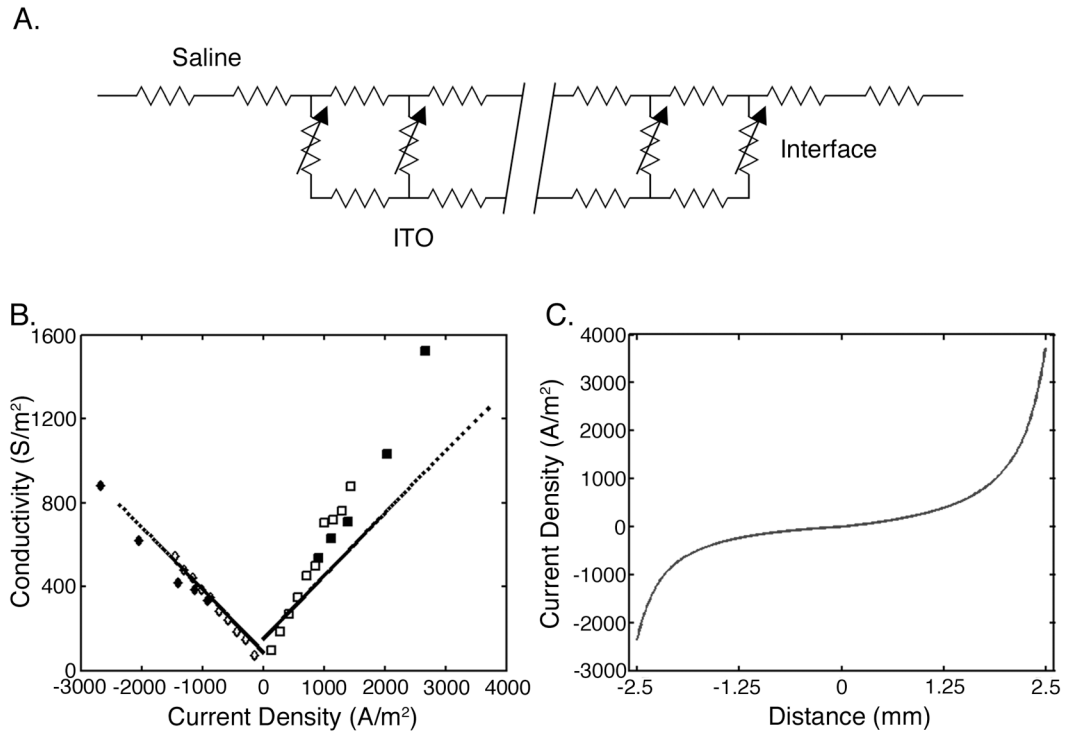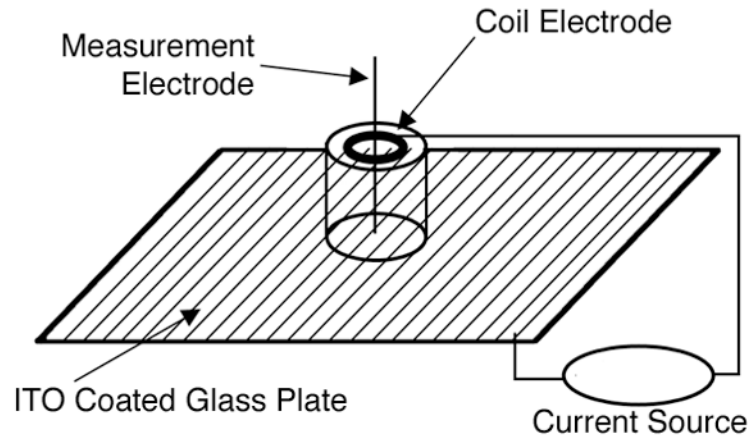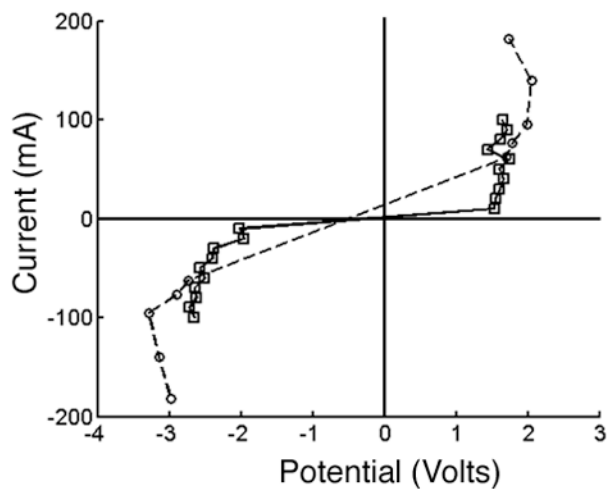
Figure 5.
Schematic of the model, conductivities and model current distribution. Panel A: Schematic diagram of the computer model. Panel B: Measurements of interfacial conductivity at various interfacial current densities from two experiments. Open symbols are measurements using Tyrode's solution and closed symbols are measurements using 0.9 % sodium chloride solution. The ITO was the anode for results on the left (diamonds), and was the cathode for results on the right (squares). The dots represent the relationship between the conductivity and the current density at interfacial elements in the model. Panel C: Model Current densities at the interface of a 5 mm wide ITO conductor with a solution are shown as a function of distance from the center of the conductor in the direction perpendicular to shock electrodes. Anodal half is to the left and cathodal half is to the right.
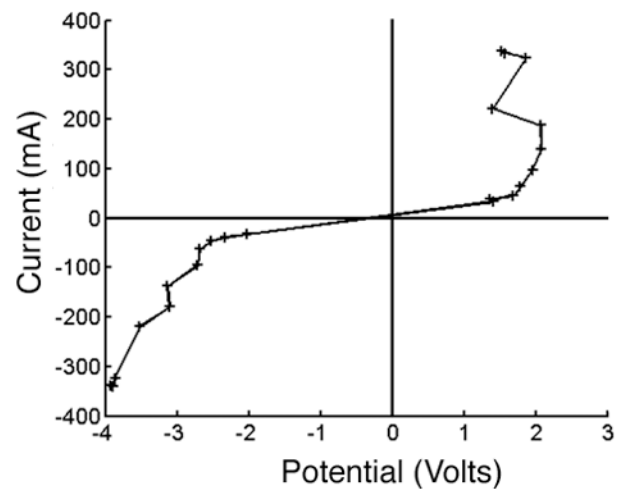
A.

B.

C.

Figure 6.
Panel A: Diagram of the experimental setup used to measure interfacial conductivity. A 9.4 mm diameter chamber was cemented to an indium-tin-oxide (ITO)-coated glass plate. Current was sent between the ITO and the coil electrode. Voltages were measured between the ITO and the measurement electrode. Panels B and C: Measurements of the relationship between interfacial current and voltage. The ITO was the anode for results on the left, and was the cathode for results on the right.
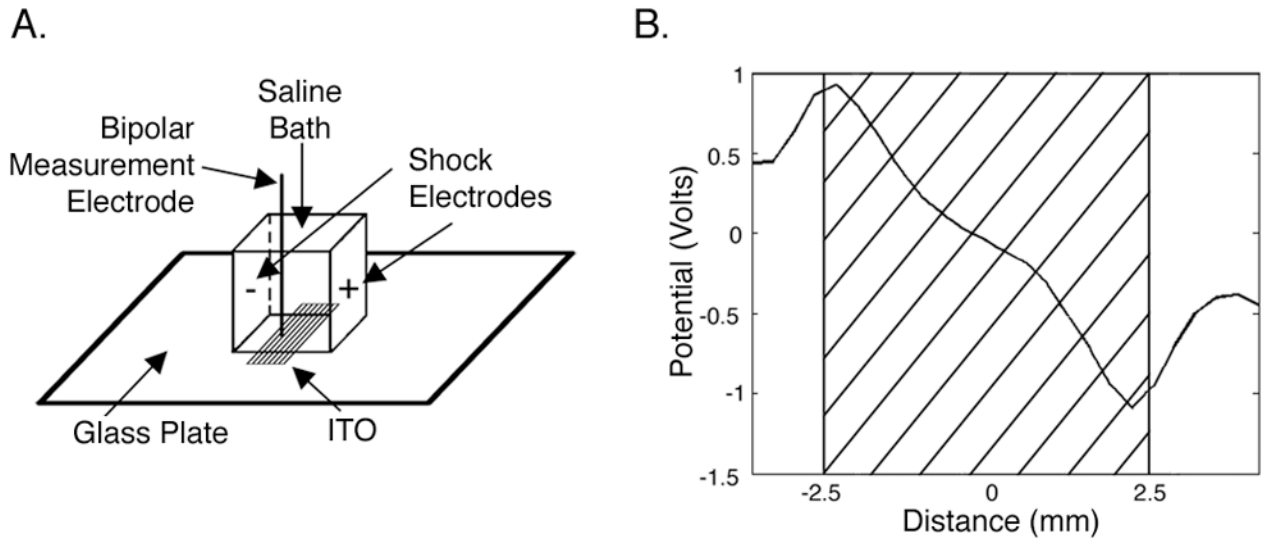
Figure 7.
Vertical component of potential differences measured with roving bipolar electrode above indium tin oxide (ITO) during shocks. Panel A: Diagram of experimental setup. The glass plate with a 5-mm wide ITO conductor was cemented to saline filled chamber. The shock electrodes were at opposite sides. The bipolar electrode scanned from cathodal shock electrode toward anodal shock electrode. Panel B: Potential differences shown as a function of position of bipolar electrode. Approximate ITO location is indicated (hatched area).
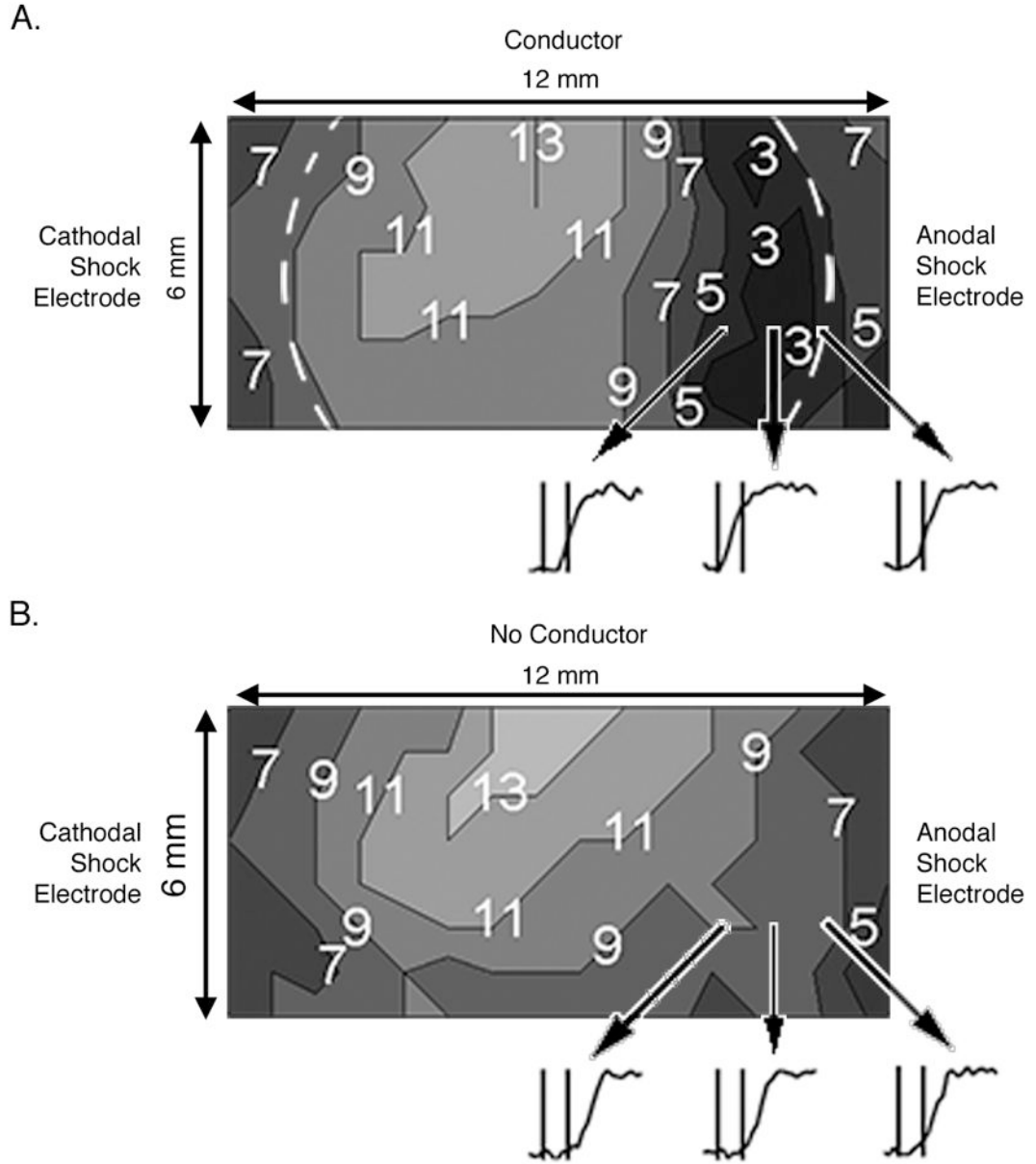
Figure 8.
Excitation isochrone contour maps and ratiometric fluorescence recordings of phase zero depolarizations produced by electric field stimulation with and without a circular indium-tin-oxide (ITO) conductor on rabbit ventricular epicardium. The location of the conductor is shown by the dotted line. Vertical lines on each recording indicate times of onset and termination of shock. Strength of current applied from shock electrodes was 62 mA. Excitation times in the mapped region are given in msec relative to onset of shock. Edge of ITO conductor facing anodal shock electrode was within 1 mm from the site of earliest excitation in Panel A.